Chapter 10

ZnO-Based Electron Transporting Layer for Perovskite Solar Cells

Lung-Chien Chen and Zong-Liang Tseng

Additional information is available at the end of the chapter

http://dx.doi.org/10.5772/65056

Abstract

Recently, organic/inorganic hybrid perovskite materials, $APbX_3$ (A = CH_3NH_3 or $HC(NH_2)_2$; X = I, Br or Cl), have attracted much interest for their promising application in solar cells as the light-absorbing component to their broad spectral absorption, strong light-harvesting and long exciton diffusion length. The perovskite solar cells (PSCs) can reduce the production costs and achieve high power conversion efficiency significantly compared to standard silicon cells and other thin film cells. On the other hand, ZnO based materials have been recently investigated in the PSCs devices as electron injection layers for low-temperature, low-cost and flexible devices. This chapter aims to review PSCs using ZnO materials as electron extraction layers. We will discuss the electron transmission and effect of the electron-transporting layer in PSCs and the preparation method of the ZnO. ZnO is a potential material for many applications due to their high electron mobility, transparent and various nanostructure. The ZnO was introduced into the PSCs structure to improve electron extraction efficiency. This chapter summaries the effect and parameters of PSCs based on the ZnO layer/nanostructure prepared by several methods as electron transport layers.

Keywords: perovskite, solar cell, ZnO, photovoltaic, hybrid

1. Introduction

Lead halide perovskites materials have been well known for many years [1], but the first incorporation into photovoltaic applications was reported by Miyasaka et al. in 2009 [2]. The lead halide perovskites, $CH_3NH_3PbBr_3$, and $CH_3NH_3PbI_3$ were coated on a mesoporous TiO_2 electron-collector as photosensitized dyes and generated 3.8% power conversion efficiency (PCE), which was based on a dye-sensitized solar cell (DSSC) architecture. However, the cells

were only stable for a matter of minutes because of a liquid corrosive electrolyte. In 2009, using the same dye-sensitized concept to improve upon the PCE, achieving 6.5% PCE [3].

In general, the word "perovskite" is used to describe any material with the same structure as inorganic $CaTiO_3$. Organic halide perovskites present a general formula of AMX_3, where A and M are monovalent and bivalent cations, respectively, and X is a monovalent anion that binds to both cations. M is coordinated to six X anions, and A is coordinated to 12 X anions (**Figure 1**). Consequently, they form anionic M-X semiconducting frameworks and charge-compensating cations [1]. In this case of lead halide perovskites, M is Pb atom and X is a halogen atom (Cl, Br, I, or a combination of them). The PbX_6 octahedra consists of a three-dimensional (3D) framework and small-sized organic or inorganic cations, which can fit into the PbX_6 framework, such as $CH_3NH_3^+$, $HC(NH_2)_2^+$, and Cs+.

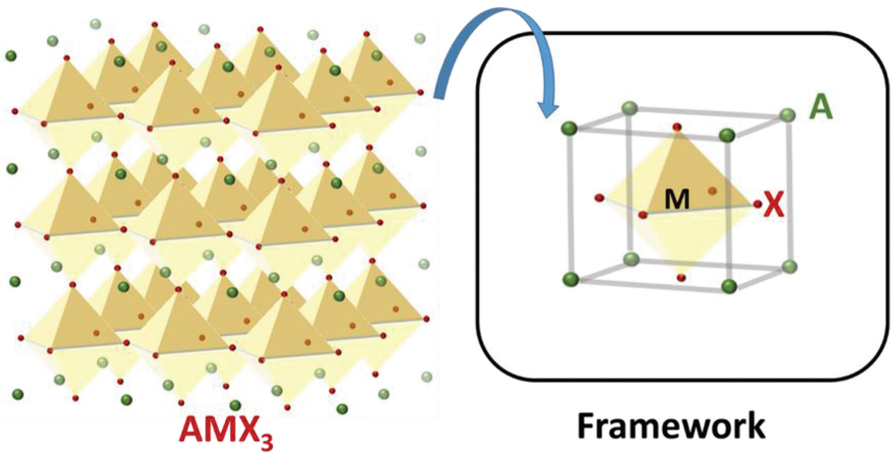

Figure 1. Schematic representation of the 3D inorganic framework of organic halide perovskites.

A breakthrough came in 2012, Michael Grätzel and Park [4] contacted $CH_3NH_3PbI_3$ perovskites with a solid-state electrolyte, spiro-OMeTAD, as a hole-transporting layer (HTL) to improve the device stability. The device structure is shown in **Figure 2**. The all-solid-state mesoscopic solar cells showed the PCE exceeding 9% and began a new perovskite solar cell (PSC) subject in the photovoltaic researches. Subsequently, Lee et al. [5], from the University of Oxford, replaced the mesoporous TiO_2 with an inert Al_2O_3 scaffold, resulting in increased open-circuit voltage and a relative improvement in efficiency of 3–5% more than those with TiO_2 scaffolds, as shown in **Figure 3** [4]. One cell of Al_2O_3-based cells exhibited high efficiency (red solid trace with crosses) and one exhibiting Voc > 1.1 V (red dashed line with crosses); for a perovskite-sensitized TiO_2 solar cell (black trace with circles); and for a planar-junction diode with structure FTO / compact TiO2 / $CH_3NH_3PbI_{3-x}Cl_x$ / spiro-OMeTAD / Ag (purple trace with squares). They showed that the efficiencies of almost 10% were achievable using the 'sensitized' TiO_2 architecture with the solid-state hole transporter, but higher efficiencies, above 10%, were attained by replacing it with an inert scaffold. This showed the PSCs may not require the mesoporous TiO_2 layer in order to transport electrons and the hypothesis that a scaffold is not needed for electron extraction was proved later. A thin-film type PSCs, with no mesoporous scaffold, of >10% efficiency were achieved [6–9].

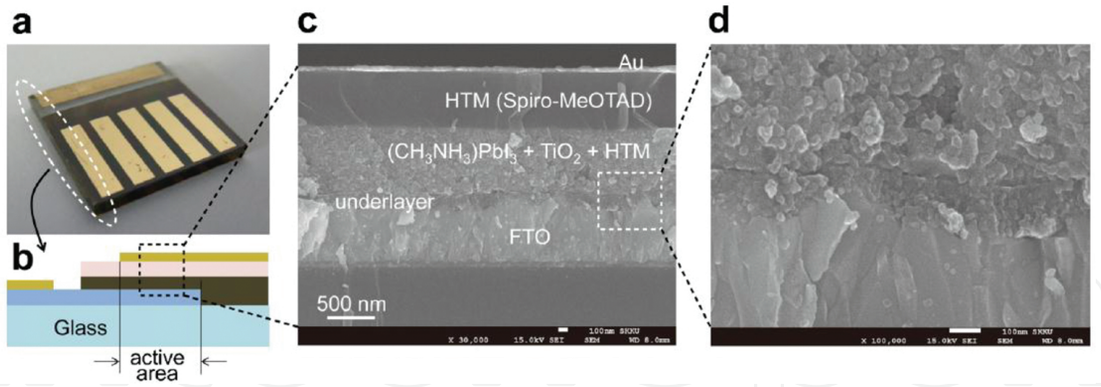

Figure 2. Solid-state device and its cross-sectional mesostructure. (a) Real solid-state device. (b) Cross-sectional structure of the device. (c) Cross-sectional SEM image of the device. (d) Active layer-underlayer-FTO interfacial junction structure.

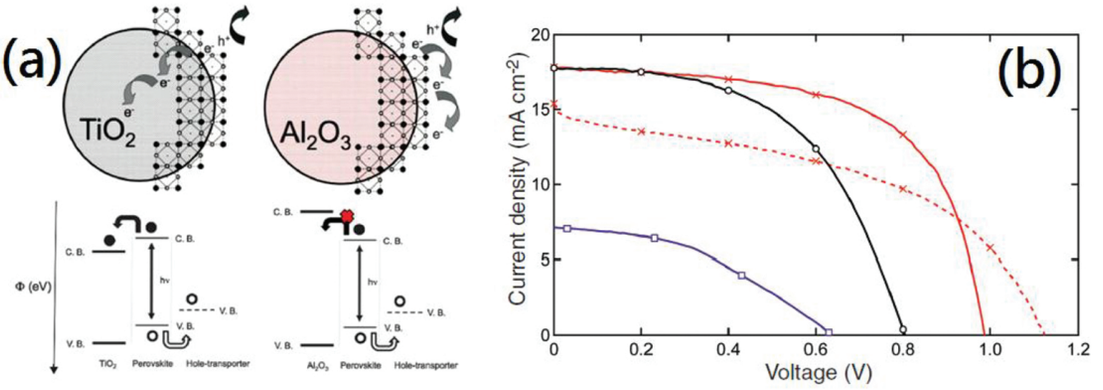

Figure 3. (a) Schematic illustrating the charge transfer and charge transport in a perovskite-sensitized TiO_2 solar cell (left) and a noninjecting Al_2O_3-based solar cell (right). (b) Current density-voltage characteristics under simulated AM1.5 illumination for Al_2O_3-based cells, one cell exhibiting high efficiency (red solid trace with crosses) and one exhibiting VOC > 1.1 V (red dashed line with crosses); for a perovskite-sensitized TiO_2 solar cell (black trace with circles); and for a planar-junction diode with structure FTO/compact TiO_2/$CH_3NH_3PbI_2Cl$/spiro-OMeTAD/Ag (purple trace with squares).

In 2013, both the planar and mesoscopic architectures, **Figure 4**, saw a large amount of developments. Burschka et al. [10] and Bi et al. [11] demonstrated a deposition technique for the mesoscopic-type architecture, exceeding 15% efficiency using a two-step solution processing; Liu et al. [12] showed that it was possible to fabricate planar-type PSCs; using thermal evaporation method at a similar time, over 15% efficiency was achieved. A number of new deposition techniques and even higher efficiencies were reported in 2014 [13, 14]. A reverse-scan efficiency of 19.3% was claimed by Zhou et al. [15] at UCLA using the planar thin-film architecture. In November 2014, a device by researchers from KRICT achieved a record with the certification of a non-stabilized efficiency of 20.1% [15, 16]. In December 2015, a new record efficiency of 21.0% was achieved by EPFL [15]. Subsequently, in March 2016, researchers from KRICT and UNIST created the highest certified record for a single-junction perovskite solar cell with 22.1% [15].

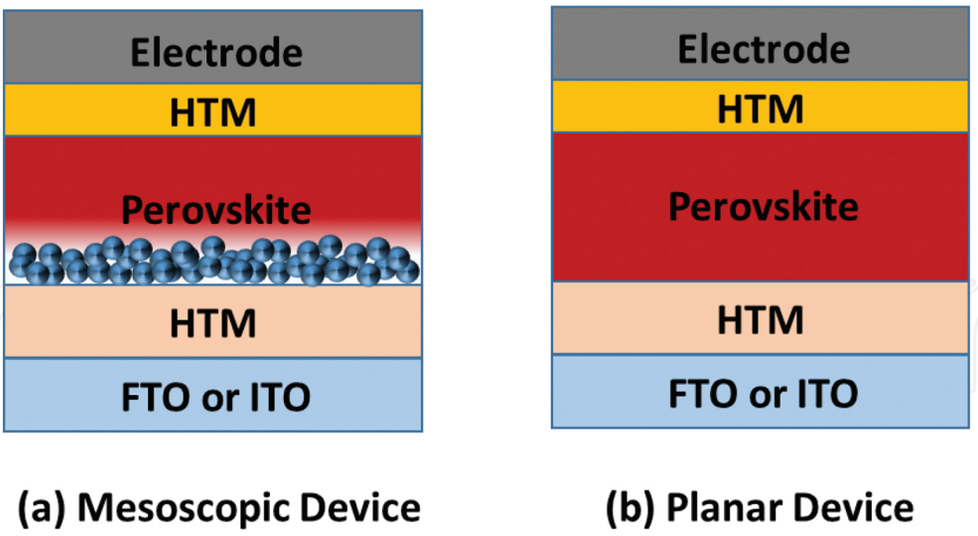

Figure 4. Structure diagram of (a) mesoscopic perovskite solar cell and (b) planar perovskite solar cell.

2. Electron transporting layer in perovskite solar cells

The electron-transporting layer (ETL), one of the most important components in the PSCs for highly efficient performance, plays an essential role in extracting and transporting photogenerated electrons. Simultaneously, it also serves as a hole-blocking layer to suppress carrier recombination. The characteristics of the ETL, especially its carrier mobility, energy band alignment, morphology, trap states, and related interfacial properties are major factors to determine the device behavior and photovoltaic performance of PSCs [17]. A relatively high electron mobility is desirable for ETLs to efficiently transport and collect electrons transport, contributing to the increase of short-circuit current density (Jsc), and fill factor (FF). The better matching energy level between ETLs and the perovskite layer can facilitate electron extraction and transport. Furthermore, the open-circuit voltage (Voc) can be determined by the energy level differences between the Fermi levels (EF) of the ETL and EF of the hole-transporting layer (HTL) [18–20]. Hence, the energy-level engineering is widely used to improve the Voc of a photovoltaic device. Trap states in the ETLs also play important roles in charge transport. Therefore, improving interface contact between ETLs and the perovskite layer is an efficient method to optimize device performance and enhance charge transport. Morphologies of the ETL are also considered to enhance its contact with the perovskite layer for achieving better device behavior.

To date, TiO_2 materials have been used as ETLs in most frequently reported PSCs. The electron injection rates between the perovskite absorber and TiO_2 ETLs are very fast, but the high electron recombination rates are also seen due to the low electron mobility and transporting properties [21]. In addition, a high-temperature process was required for high-quality mesoscopic TiO_2 layer [16, 22]. Hence, these characteristics of TiO_2 materials may act as impediments to improve device performance and their further application for developing low-cost perov-

http://dx.doi.org/10.5772/65056

skite solar cells on various flexible substrates [23, 24]. On the other hand, ZnO is a wide-bandgap semiconductor of the II-VI semiconductor group, which has several favorable properties, including good transparency, high electron mobility, wide bandgap, and strong room-temperature luminescence. Several types of morphologies in ZnO, such as thin film, single-crystal, nanowire, and nanorod has been found and made using the low-temperature solution processes. The native doping of the semiconductor due to oxygen vacancies or zinc interstitials is n-type [25]. Moreover, ZnO is a well-known material that has similar energy level as TiO_2 but has better electron mobility (bulk mobility: 200–300 cm^2/V s [25–27]) than TiO_2, which lets it an ideal candidate for a low-temperature processed electron-selective contact for transparent electrodes, organic solar cell, thin-film transistors, and light-emitting diodes.

3. ZnO film/nanostructure as electron transporting layer

In 2013, ZnO was firstly applied as ETL of PSCs. Kumar et al. [28] reported flexible PSCs employing the ZnO compact layer as a hole-blocking layer and a ZnO nanorods mesoscopic scaffold layer as an electron transporter. The ZnO compact layer was formed by electrodeposition and ZnO nanorods grown by chemical bath deposition, which allow the processing of low-temperature, solution-based ETLs. The planar device, which only uses the ZnO compact layer can also be made, but they presented lower Jsc and FF than nanorod-based devices. Conversion efficiencies of 8.90% were achieved on rigid substrates, while the flexible ones yielded 2.62%. In the same year, Bi et al. [29] used well-aligned ZnO nanorod arrays as ETLs. They consider that the perovskite material has better solar cell stability and is therefore more suited as a sensitizer for ZnO nanorod arrays. Therefore, their results showed the ZnO nanorod-based PSCs had a good long-term stability of PSCs. It was found that the electron transport time and lifetime vary with the ZnO nanorod length, a trend which is similar to that in DSSCs, suggesting a similar charge transfer process in the ZnO nanorod array/$CH_3NH_3PbI_3$ interface as in conventional DSSCs. However, a solar cell efficiency of only 5.0% was achieved under AM 1.5 G illumination due to more recombination losses than TiO_2 devices. The reason indicated that the ZnO nanorod array grown by different processes may affect the PSC performance.

A breakthrough came in the end of 2013, Liu and Kelly [30] reported that a room temperature solution-processed thin compact ZnO ETL was used to fabricate a highly efficient planar perovskite solar cell with a champion efficiency of 15.7%, an average efficiency of 13.7%, and the flexible ones yielded 10.2%, in which ZnO prepared by a co-precipitation method had superior electron mobility, and the ETLs were fabricated without any sintering steps, as shown in **Figure 5**. Besides solution-based co-precipitation ZnO ETLs, a sol-gel solution-processed ZnO ETLs were reported by Kim et al. [31] in 2014. Moreover, a vacuum-processed ZnO ETL has been prepared for high-efficiency PSCs, such as an atom layer deposition (ALD) [32] or sputtering method [33, 34]. Several types of ZnO nanostructures have been studied to replace the mesoporous TiO_2 nanostructures in the conventional PSCs [35–38].

On the other hand, the electrical characteristics of ZnO can be increased by extrinsically doping a small amount of impurities [39, 40], such as Al. The ionic radius of Al^{3+} is 0.54 Å, which is smaller than that of Zn^{2+} (0.74 Å). Therefore, Al^{3+} can replace Zn^{2+} in the lattice point and acts as a donor to increase the conductivity of ZnO [41, 42], and at the same time, it remains the excellent transparence in the visible-light region. This is why a high-quality Al-doped ZnO (AZO) thin film can also be used as a transparent conductive oxide (TCO) electrode, just like other IIIA elements (B, Ga, and In)-doped ZnO [41]. Al-doped ZnO thin film, which was deposited using the electrospraying method, was also used as ETLs in PSCs to suppress charge recombination at the ZnO/perovskite interface, resulting in better efficiency than pure ZnO devices [43]. The charge recombination of the ZnO-based device was also suppressed by appropriate Mg-doping. It mainly attributed to the conduction band offset at the interface between ZnO ETL and perovskite layer [44].

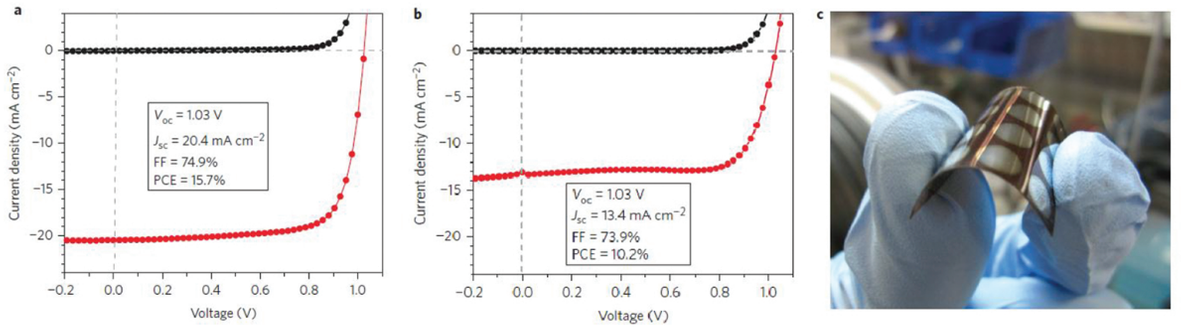

Figure 5. J–V curves of devices on (a) glass and (b) flexible PET substrates in the illumination (red line) and dark (black line) for the highest-performing ITO/ZnO/$CH_3NH_3PbI_3$/spiro-OMeTAD/Ag devices in reference [31]. (c) Photograph of a device prepared on a flexible PET substrate.

The electron extraction by the ETL in perovskite cell strongly depends on the work function (WF) of the ETL. An energy barrier mismatch (a Schottky barrier) between the WF of the ETL and the lowest unoccupied molecular orbital (LUMO) of perovskite absorber could lead to inefficient electron extraction. Therefore, matching the WF of ETL with the absorber could reduce a Schottky barrier or form an Ohmic contact [45, 46] to facilitate the electron injection or collection [47]. Nitrogen-doped ZnO electron materials combined with a dipole layer can increase electron concentration to improve perovskite infiltration and reduce the work function [38]. Above all, doping is an effective way to modify the electrical properties of ZnO.

Self-assembled monolayer (SAM) is well-known that surface treatments can decrease the number of charge carrier traps and tune the surface WF of ETLs. Modification of the interface of solar cells using functional SAMs is an effective method to improve device performance. Modifying the ZnO ETL with 3-aminopropanoic acid monolayer can improve the interfacial energy level alignment due to the formation of permanent dipole moments, which decreased the WF of ZnO from 4.17 to 3.52 eV, and help to obtain highly crystalline perovskite layer with reduced pin-hole and trap-state density [48]. The stoichiometry of ZnO thin film was also affected the photovoltaic device performance. Tseng et al. [33] used sputtered ZnO thin films, which stoichiometry was controlled by adjusting the ratio of working gases (Ar and O_2) during

http://dx.doi.org/10.5772/65056

radio frequency (RF) magnetron-sputtering process, as an ETL in PSCs. As mentioned earlier, the native doping of the ZnO due to oxygen vacancies shows n-type semiconductor. The surface conductivity of ZnO film was affected by the presence of oxygen vacancy of the lattice, which will show even more accentuated variations of the electrical behavior in a thin film. ZnO film with more oxygen vacancies has higher surface conductivity; therefore, device based on ZnO using pure Ar deposition has smaller series resistance. Furthermore, ZnO using pure Ar deposition has lower WF of 4.33 eV than that using Ar/O_2 mixed gas deposition (4.48) but both have a same bandgap. Therefore, ZnO using pure Ar deposition lower conduction band level (down-shift) than that using Ar/O_2 mixed gas deposition to increase the driven force of electron injection (or charge separation) from perovskite (or ZnO/perovskite interface) and lower valance edge can block the hole more efficiently. Both better conductivity and lower conduction band level of ZnO result in high charge extraction efficient; therefore, the corresponding device has high Jsc. (**Figure 6a** and **b**) The hole-blocking ability of ZnO film using pure Ar deposition was also supported by the dark current of the corresponding device illustrated in **Figure 6c**. Cell-based ZnO-Ar electron-transporting layer has smaller dark current indicated that ZnO-Ar has better hole-blocking ability when other components in the cell are supposed to be the same.

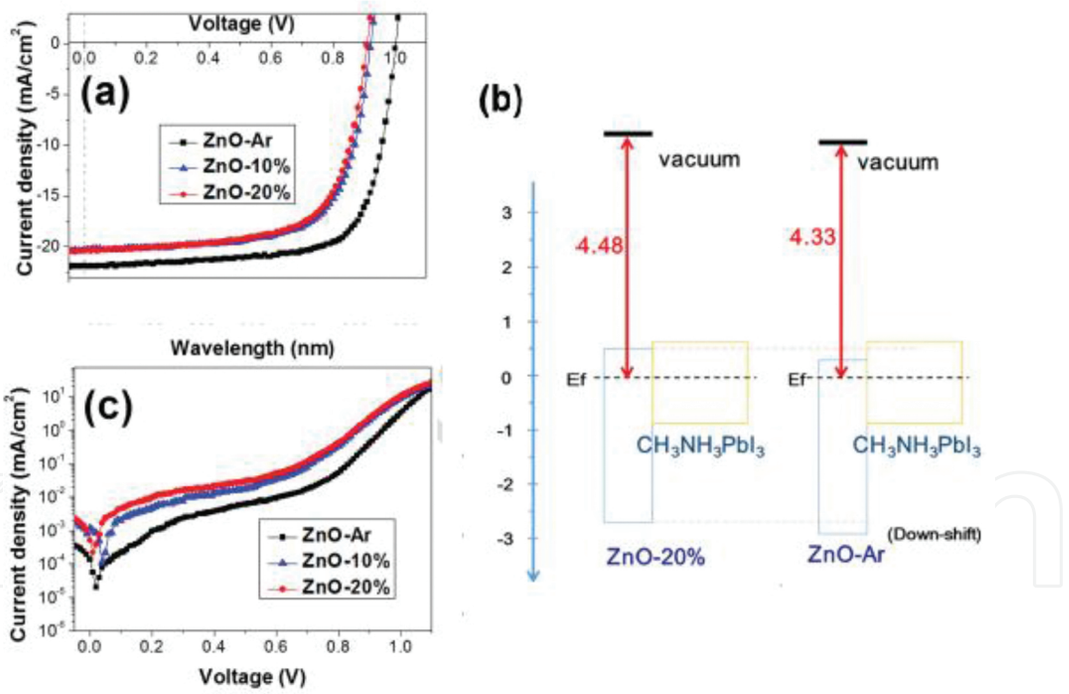

Figure 6. (a) I-V curves, (b) illustration of the frontier orbitals energy levels for ZnO prepared using pure Ar and 20% O_2, and (c) Dark current curves of perovskite solar cell using pure Ar, 10%, and 20% Ar/Ar + O_2 ratio mixed gas as the electron transport layer. The illustration of the frontier orbitals energy levels for ZnO-Ar, ZnO-20%, and perovskite.

Despite the excellent characteristics of ZnO, in 2015, Yang et al. [49] found the thermal instability of PSCs fabricated using ZnO ETLs. They show that the basic nature of the ZnO surface leads to proton-transfer reactions at the ZnO/$CH_3NH_3PbI_3$ interface, which results in

decomposition of the perovskite film PbI_2, as shown in **Figure 7**. The decomposition process is accelerated by the presence of surface hydroxyl groups and/or residual acetate ligands. To reduce the decomposition, Cheng et al. [50] introduced a buffer layer in between the ZnO-NPs and perovskite layers. They found that a commonly used buffer layer with small molecule like [6,6]-phenyl-C_{61}-butyric acid methyl ester (PCBM) can slow down but cannot avoid the decomposition completely. On the other hand, a polymeric buffer layer using poly(ethylenimine) (PEI) can effectively separate the ZnO-NPs and perovskite, which allows larger crystal formation with thermal annealing. Today, thermal instability of PSCs using ZnO ETLs remains the major challenge limiting their further application and device performance.

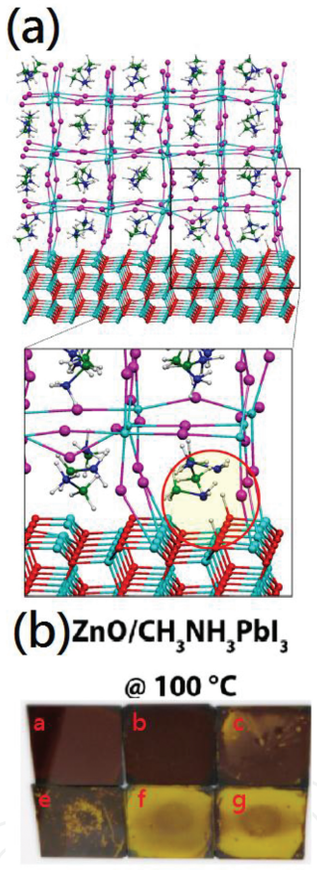

Figure 7. (a) Optimized geometrical structure of the $ZnO/CH_3NH_3PbI_3$ interface. The inset shows a magnified view of the deprotonated methylammonium cations. (b) Photographs of $CH_3NH_3PbI_3$ films deposited on ZnO layers and heated to 100°C with different times (from a to g).

4. Conclusions

In summary, we have given an overview of the efforts focused on the ZnO of ETLs. Their doping effect and interface modification between the ETL and perovskite layer have been developed and applied in PSCs. Because charge extraction, transfer, and recombination mainly occur at

the interfaces of a cell, the interfacial layer between the perovskite layer and the bottom electrode needs to be closely aligned by introducing efficient interfacial materials. For conventional PSCs, a ZnO ETL, good electron-transport ability and a low recombination rate at the interface, works well for high-performance PSC.

Author details

Lung-Chien Chen* and Zong-Liang Tseng

*Address all correspondence to: ocean@ntut.edu.tw

Department of Electro-Optical Engineering, National Taipei University of Technology, Taipei, Taiwan

References

[1] S. Dastidar, Egger, D. A., Tan, L. Z., Cromer, S. B., Dillon, A. D., Liu, S., Kronik, L., Rappe, A. M., Fafarman, A. T. High chloride doping levels stabilize the perovskite phase of cesium lead iodide. Nano Letters. 2016; 16(6), 3563–3570. doi:10.1021/acs.nanolett.6b00635

[2] A. Kojima, Teshima, K., Shirai, Y., Miyasaka, T. Organometal halide perovskites as visible-light sensitizers for photovoltaic cells. Journal of the American Chemical Society. 2009; 131(17), 6050–6051. doi:10.1021/ja809598r

[3] J.-H. Im, Lee, C.-R., Lee, J.-W., Park, S.-W., Park, N.-G. 6.5% efficient perovskite quantum-dot-sensitized solar cell. Nanoscale. 2011; 3(10), 4088–4093. doi:10.1039/C1NR10867K

[4] H.-S. Kim, Lee, C.-R., Im, J.-H., Lee, K.-B., Moehl, T., Marchioro, A., Moon, S.-J., Humphry-Baker, R., Yum, J.-H., Moser, J. E., Grätzel, M., Park, N. G. Lead iodide perovskite sensitized all-solid-state submicron thin film mesoscopic solar cell with efficiency exceeding 9%. Scientific Reports. 2012; 2, doi:10.1038/srep00591

[5] M. M. Lee, Teuscher, J., Miyasaka, T., Murakami, T. N., Snaith, H. J. Efficient hybrid solar cells based on meso-superstructured organometal halide perovskites. Science. 2012; 338(6107), 643–647. doi:10.1126/science.1228604

[6] G. E. Eperon, Burlakov, V. M., Docampo, P., Goriely, A., Snaith, H. J. Morphological control for high performance, solution-processed planar heterojunction perovskite solar cells. Advanced Functional Materials. 2014; 24(1), 151–157. doi:10.1002/adfm.201302090

[7] M. Saliba, Tan, K. W., Sai, H., Moore, D. T., Scott, T., Zhang, W., Estroff, L. A., Wiesner, U., Snaith, H. J. Influence of thermal processing protocol upon the crystallization and

photovoltaic performance of organic–inorganic lead trihalide perovskites. The Journal of Physical Chemistry C. 2014; 118(30), 17171–17177. doi:10.1021/jp500717w

[8] K. W. Tan, Moore, D. T., Saliba, M., Sai, H., Estroff, L. A., Hanrath, T., Snaith, H. J., Wiesner, U. Thermally induced structural evolution and performance of mesoporous block copolymer-directed alumina perovskite solar cells. ACS Nano. 2014; 8 (5), 4730–4739. doi:10.1021/nn500526t

[9] J. M. Ball, Lee, M. M., Hey, A., Snaith, H. J. Low-temperature processed meso-superstructured to thin-film perovskite solar cells. Energy and Environmental Science. 2013; 6(6), 1739–1743. doi:10.1039/C3EE40810H

[10] J. Burschka, Pellet, N., Moon, S.-J., Humphry-Baker, R., Gao, P., Nazeeruddin, M. K., Gratzel, M. Sequential deposition as a route to high-performance perovskite-sensitized solar cells. Nature. 2013; 499(7458), 316–319. doi:10.1038/nature12340

[11] D. Bi, Moon, S.-J., Haggman, L., Boschloo, G., Yang, L., Johansson, E. M. J., Nazeeruddin, M. K., Gratzel, M., Hagfeldt, A. Using a two-step deposition technique to prepare perovskite ($CH_3NH_3PbI_3$) for thin film solar cells based on ZrO_2 and TiO_2 mesostructures. RSC Advances. 2013; 3 (41), 18762–18766. doi:10.1039/C3RA43228A

[12] M. Liu, Johnston, M. B., Snaith, H. J. Efficient planar heterojunction perovskite solar cells by vapour deposition. Nature. 2013; 501(7467), 395–398. doi:10.1038/nature12509

[13] Wikipedia. Perovskite solar cell [Internet]. 2016. Available from: https://en.wikipedia.org/wiki/Perovskite_solar_cell

[14] NREL. Research Cell efficiency records [Internet]. 2016. Available from: http://www.nrel.gov/ncpv/images/efficiency_chart.jpg

[15] H. Zhou, Chen, Q., Li, G., Luo, S., Song, T.-b., Duan, H.-S., Hong, Z., You, J., Liu, Y., Yang, Y. Interface engineering of highly efficient perovskite solar cells. Science. 2014; 345(6196), 542–546. doi:10.1126/science.1254050

[16] W. S. Yang, Noh, J. H., Jeon, N. J., Kim, Y. C., Ryu, S., Seo, J., Seok, S. I. High-performance photovoltaic perovskite layers fabricated through intramolecular exchange. Science. 2015; 348(6240), 1234–1237. doi:10.1126/science.aaa9272

[17] G. Yang, Tao, H., Qin, P., Ke, W., Fang, G. Recent progress in electron transport layers for efficient perovskite solar cells. Journal of Materials Chemistry A. 2016; 4(11), 3970–3990. doi:10.1039/C5TA09011C

[18] S. Ryu, Noh, J. H., Jeon, N. J., Kim, Y. C., Yang, W. S., Seo, J., Seok, S. I. Voltage output of efficient perovskite solar cells with high open-circuit voltage and fill factor. Energy and Environmental Science. 2014; 7(8), 2614–2618. doi:10.1039/C4EE00762J

[19] A. R. b. M. Yusoff, Nazeeruddin, M. K. Organohalide lead perovskites for photovoltaic applications. The Journal of Physical Chemistry Letters. 2016; 7(5), 851–866. doi:10.1021/acs.jpclett.5b02893

[20] Y.-F. Chiang, Jeng, J.-Y., Lee, M.-H., Peng, S.-R., Chen, P., Guo, T.-F., Wen, T.-C., Hsu, Y.-J., Hsu, C.-M. High voltage and efficient bilayer heterojunction solar cells based on an organic-inorganic hybrid perovskite absorber with a low-cost flexible substrate. Physical Chemistry Chemical Physics. 2014; 16(13), 6033–6040. doi:10.1039/C4CP00298A

[21] S. Gubbala, Chakrapani, V., Kumar, V., Sunkara, M. K. Band-edge engineered hybrid structures for dye-sensitized solar cells based on SnO_2 nanowires. Advanced Functional Materials. 2008; 18(16), 2411–2418. doi:10.1002/adfm.200800099

[22] N. J. Jeon, Noh, J. H., Yang, W. S., Kim, Y. C., Ryu, S., Seo, J., Seok, S. I. Compositional engineering of perovskite materials for high-performance solar cells. Nature. 2015; 517(7535), 476–480. doi:10.1038/nature14133

[23] Z. M. Beiley, McGehee, M. D. Modeling low cost hybrid tandem photovoltaics with the potential for efficiencies exceeding 20%. Energy and Environmental Science. 2012; 5(11), 9173–9179. doi:10.1039/C2EE23073A

[24] C. Roldan-Carmona, Malinkiewicz, O., Soriano, A., Minguez Espallargas, G., Garcia, A., Reinecke, P., Kroyer, T., Dar, M. I., Nazeeruddin, M. K., Bolink, H. J. Flexible high efficiency perovskite solar cells. Energy and Environmental Science. 2014; 7(3), 994–997. doi:10.1039/C3EE43619E

[25] Ü. Özgür, Alivov, Y. I., Liu, C., Teke, A., Reshchikov, M. A., Doğan, S., Avrutin, V., Cho, S.-J., Morkoç, H. A comprehensive review of ZnO materials and devices. Journal of Applied Physics. 2005; 98(4), 041301. doi:10.1063/1.1992666

[26] H. Tang, Prasad, K., Sanjinès, R., Schmid, P. E., Lévy, F. Electrical and optical properties of TiO_2 anatase thin films. Journal of Applied Physics. 1994; 75(4), 2042–2047. doi:10.1063/1.356306

[27] H. S. Bae, Yoon, M. H., Kim, J. H., Im, S. Photodetecting properties of ZnO-based thin-film transistors. Applied Physics Letters. 2003; 83(25), 5313–5315. doi:10.1063/1.1633676

[28] M. H. Kumar, Yantara, N., Dharani, S., Graetzel, M., Mhaisalkar, S., Boix, P. P., Mathews, N. Flexible, low-temperature, solution processed ZnO-based perovskite solid state solar cells. Chemical Communications. 2013; 49(94), 11089–11091. doi:10.1039/C3CC46534A

[29] D. Bi, Boschloo, G., Schwarzmuller, S., Yang, L., Johansson, E. M. J., Hagfeldt, A. Efficient and stable $CH_3NH_3PbI_3$-sensitized ZnO nanorod array solid-state solar cells. Nanoscale. 2013; 5(23), 11686–11691. doi:10.1039/C3NR01542D

[30] D. Liu, Kelly, T. L. Perovskite solar cells with a planar heterojunction structure prepared using room-temperature solution processing techniques. Nature Photonics. 2014; 8(2), 133–138. doi:10.1038/nphoton.2013.342

[31] J. Kim, Kim, G., Kim, T. K., Kwon, S., Back, H., Lee, J., Lee, S. H., Kang, H., Lee, K. Efficient planar-heterojunction perovskite solar cells achieved via interfacial modifica-

tion of a sol-gel ZnO electron collection layer. Journal of Materials Chemistry A. 2014; 2(41), 17291–17296. doi:10.1039/C4TA03954H

[32] X. Dong, Hu, H., Lin, B., Ding, J., Yuan, N. The effect of ALD-ZnO layers on the formation of $CH_3NH_3PbI_3$ with different perovskite precursors and sintering temperatures. Chemical Communications. 2014; 50(92), 14405–14408. doi:10.1039/C4CC04685D

[33] Z.-L. Tseng, Chiang, C.-H., Wu, C.-G. Surface engineering of ZnO thin film for high efficiency planar perovskite solar cells. Scientific Reports. 2015; 5, doi:13211.10.1038/srep13211

[34] L. Liang, Huang, Z., Cai, L., Chen, W., Wang, B., Chen, K., Bai, H., Tian, Q., Fan, B. Magnetron sputtered zinc oxide nanorods as thickness-insensitive cathode interlayer for perovskite planar-heterojunction solar cells. ACS Applied Materials and Interfaces. 2014; 6(23), 20585–20589. doi:10.1021/am506672j

[35] J. Zhang, Barboux, P., Pauporté, T. Electrochemical design of nanostructured ZnO charge carrier layers for efficient solid-state perovskite-sensitized solar cells. Advanced Energy Materials. 2014; 4(18), doi:10.1002/aenm.201400932

[36] D.-Y. Son, Im, J.-H., Kim, H.-S., Park, N.-G. 11% efficient perovskite solar cell based on ZnO nanorods: an effective charge collection system. The Journal of Physical Chemistry C. 2014; 118(30), 16567–16573. doi:10.1021/jp412407j

[37] A. K. Chandiran, Abdi-Jalebi, M., Yella, A., Dar, M. I., Yi, C., Shivashankar, S. A., Nazeeruddin, M. K., Grätzel, M. Quantum-confined ZnO nanoshell photoanodes for mesoscopic solar cells. Nano Letters. 2014; 14(3), 1190–1195. doi:10.1021/nl4039955

[38] K. Mahmood, Swain, B. S., Amassian, A. 16.1% efficient hysteresis-free mesostructured perovskite solar cells based on synergistically improved ZnO nanorod arrays. Advanced Energy Materials. 2015; 5(17), doi:10.1002/aenm.201500568

[39] E. Klaus. Magnetron sputtering of transparent conductive zinc oxide: relation between the sputtering parameters and the electronic properties. Journal of Physics D: Applied Physics. 2000; 33(4), R17–R32. doi:http://iopscience.iop.org/0022-3727/33/4/201

[40] Liu, Y., Li, Y..Zeng, H. ZnO-Based Transparent Conductive Thin Films: Doping, Performance, and Processing. Journal of Nanomaterials. 2013; 2013, 196521. DOI: http://dx.doi.org/10.1155/2013/196521.

[41] Sans, J. A., Sánchez-Royo, J. F., Segura, A., Tobias, G..Canadell, E. Chemical effects on the optical band-gap of heavily doped ZnO:MIII (M = Al, Ga, In): An investigation by means of photoelectron spectroscopy, optical measurements under pressure, and band structure calculations. Physical Review B. 2009; 79 (19), 195105. DOI: http://dx.doi.org/10.1103/PhysRevB.79.195105

[42] J. L. Zhao, Sun, X. W., Ryu, H., Moon, Y. B. Thermally stable transparent conducting and highly infrared reflective Ga-doped ZnO thin films by metal organic chemical

vapor deposition. Optical Materials. 2011; 33(6), 768–772. doi:10.1016/j.optmat.2010.12.008

[43] K. Mahmood, Swain, B. S., Jung, H. S. Controlling the surface nanostructure of ZnO and Al-doped ZnO thin films using electrostatic spraying for their application in 12% efficient perovskite solar cells. Nanoscale. 2014; 6(15), 9127–9138. doi:10.1039/C4NR02065K

[44] J. Dong, Shi, J., Li, D., Luo, Y., Meng, Q. Controlling the conduction band offset for highly efficient ZnO nanorods based perovskite solar cell. Applied Physics Letters. 2015; 107(7), 073507. doi:10.1063/1.4929435

[45] H. Kang, Hong, S., Lee, J., Lee, K. Electrostatically self-assembled nonconjugated polyelectrolytes as an ideal interfacial layer for inverted polymer solar cells. Advanced Materials. 2012; 24(22), 3005–3009. doi:10.1002/adma.201200594

[46] J. C. Yu, Kim, D. B., Baek, G., Lee, B. R., Jung, E. D., Lee, S., Chu, J. H., Lee, D.-K., Choi, K. J., Cho, S., Song, M. H. High-performance planar perovskite optoelectronic devices: a morphological and interfacial control by polar solvent treatment. Advanced Materials. 2015; 27(23), 3492–3500. doi:10.1002/adma.201500465

[47] Y. Zhou, Fuentes-Hernandez, C., Shim, J., Meyer, J., Giordano, A. J., Li, H., Winget, P., Papadopoulos, T., Cheun, H., Kim, J., Fenoll, M., Dindar, A., Haske, W., Najafabadi, E., Khan, T. M., Sojoudi, H., Barlow, S., Graham, S., Brédas, J.-L., Marder, S. R., Kahn, A., Kippelen, B. A universal method to produce low–work function electrodes for organic electronics. Science. 2012; 336(6079), 327–332. doi:10.1126/science.1218829

[48] L. Zuo, Gu, Z., Ye, T., Fu, W., Wu, G., Li, H., Chen, H. Enhanced photovoltaic performance of $CH_3NH_3PbI_3$ perovskite solar cells through interfacial engineering using self-assembling monolayer. Journal of the American Chemical Society. 2015; 137(7), 2674–2679. doi:10.1021/ja512518r

[49] J. Yang, Siempelkamp, B. D., Mosconi, E., De Angelis, F., Kelly, T. L. Origin of the thermal instability in $CH_3NH_3PbI_3$ thin films deposited on ZnO. Chemistry of Materials. 2015; 27(12), 4229–4236. doi:10.1021/acs.chemmater.5b01598

[50] Y. Cheng, Yang, Q.-D., Xiao, J., Xue, Q., Li, H.-W., Guan, Z., Yip, H.-L., Tsang, S.-W. Decomposition of organometal halide perovskite films on zinc oxide nanoparticles. ACS Applied Materials and Interfaces. 2015; 7(36), 19986–19993. doi:10.1021/acsami.5b04695

IntechOpen